

Microscopic description of the anisotropy in alpha decay

D. S. Delion

Institute of Atomic Physics, Bucharest Magurele, POB MG 6, Romania

A. Insolia

Department of Physics, University of Catania and INFN, I-95129 Catania, Italy

R. J. Liotta

Royal Institute of Technology at Frescati, S-10405 Stockholm, Sweden

(Received 28 October 1993)

A microscopic description of alpha decay of odd mass nuclei is given for axially deformed nuclei. Realistic mean field+pairing residual interaction in a very large single particle basis is used. Systematics for At and Rn isotopes, as well as for ^{221}Fr , are given. A pronounced anisotropic emission of alpha particles at low temperatures is predicted as function of deformation for the At and Rn isotopes. This shows that alpha decay is an excellent tool to probe intrinsic deformations in nuclei.

PACS number(s): 23.60.+e, 21.60.Gx, 21.10.Gv, 27.90.+b

It has been shown a long time ago that in odd-mass actinides at very low temperature alpha particles are emitted preferentially with respect to the direction of the total nuclear spin [1-5]. Recently new experiments [6] have renewed the interest in this problem by reporting anisotropic emission in some near spherical At isotopes, in connection with several theoretical descriptions of this effect.

An isotropic emission of alpha particles from deformed nuclei was first explained by Hill and Wheeler [7] and later by Bohr, Fröman, and Mottelson [8] in terms of the penetration of the alpha through a deformed Coulomb barrier. It was thus found that since for a prolate nucleus the barrier at the poles is narrower than at the equator, the probability to penetrate the barrier is larger along the nuclear symmetry axis. More recently, in order to explain the observed anisotropies for near spherical At isotopes, Berggren [9] proposed an alpha+core model. A quadrupole-quadrupole interaction between the already existing structureless alpha cluster and an odd-mass core was diagonalized in a weak coupling scheme. The strength of the interaction was adjusted to obtain the energy of the emitted alpha particle. Using this model several solutions with pronounced anisotropy were obtained [10]. Buck *et al.* [11] describe alpha decay from odd-mass nuclei in a similar model, in which the depth of the alpha-core potential (taken as a square well), the alpha formation probability, and the number of nodes in the radial wave function are fitted to the experimental data. Rowley *et al.* [12] followed the same philosophy, diagonalizing the quadrupole-quadrupole interaction in an extreme cluster model basis.

In a recent series of papers [13,14] we used a realistic deformed mean field with a large configuration space+pairing residual interaction in computing the preformation amplitude of the alpha cluster inside the nucleus. We estimated the penetration through the deformed Coulomb barrier within the framework of the

Wentzel-Kramers-Brillouin (WKB) approximation. The anisotropy was explained mainly by the effect of the deformed barrier. By comparing the complete calculation with the one containing only a spherical $L=0$ component in the formation amplitude it was concluded that the anisotropy for the case of the transition $^{241}\text{Am} \rightarrow ^{237}\text{Np} + \alpha$ was changed by only 10%. Finally, the total width as well as the measured anisotropy were well reproduced in this transition.

The aim of the present paper is to continue our previous paper [14], where details of our formalism can be found, giving a systematic analysis of anisotropic alpha particle emission from odd-mass nuclei at low temperature. We also give some predictions concerning a recent proposal of experiments on anisotropy in At and Rn isotopes [15].

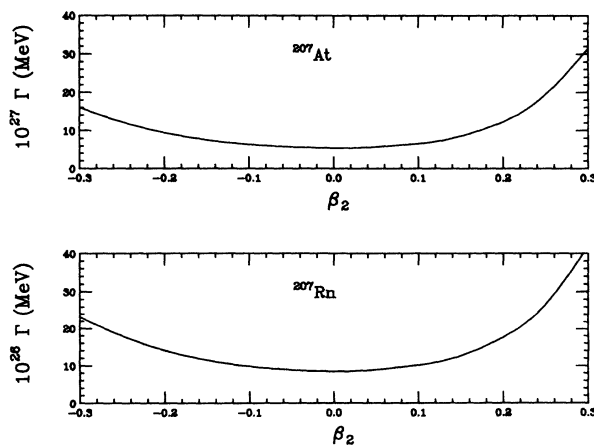


FIG. 1. Upper part: total alpha decay width versus quadrupole deformation for the odd-proton nucleus ^{207}At . Lower part: total alpha decay width versus quadrupole deformation for the odd-neutron nucleus ^{207}Rn .

TABLE I. Total widths (in MeV) in the case of At isotopes for different quadrupole deformations. Experimental widths (in MeV) from the compilation of Ref. [11].

$\beta_2 =$	-0.3	-0.2	-0.1	0.0	0.1	0.2	0.3	Γ_{exp}
$^{201}_{85}\text{At}$	1.4(-23)	8.8(-24)	6.1(-24)	5.2(-24)	6.3(-24)	1.1(-23)	2.7(-23)	3.5(-24)
$^{203}_{85}\text{At}$	1.3(-24)	7.9(-25)	5.4(-25)	4.6(-25)	5.6(-25)	1.0(-24)	2.5(-24)	3.3(-25)
$^{205}_{85}\text{At}$	1.4(-25)	8.5(-26)	5.8(-26)	4.9(-26)	6.0(-26)	1.1(-25)	2.8(-25)	2.8(-25)
$^{207}_{85}\text{At}$	1.6(-26)	9.5(-27)	6.4(-27)	5.5(-27)	6.6(-27)	1.2(-26)	3.1(-26)	6.2(-27)
$^{209}_{85}\text{At}$	5.7(-27)	3.3(-27)	2.2(-27)	1.9(-27)	2.3(-27)	4.3(-27)	1.1(-26)	0.9(-27)
$^{211}_{85}\text{At}$	1.6(-26)	9.3(-27)	6.3(-27)	5.4(-27)	6.6(-27)	1.2(-26)	3.1(-26)	7.4(-27)

In order to reproduce correctly the behavior of the formation amplitude in a region outside the nuclear surface (the asymptotic region) one needs to include very high lying single-particle states in the basis because in that region the wave functions corresponding to low-lying states are negligibly small [13]. We therefore use a harmonic oscillator basis that contains 18 major shells. The parameters of the deformed Woods-Saxon potential used in the calculations, are given in Ref. [16]. The nuclear wave functions were calculated using the Bardeen-Cooper-Schrieffer (BCS) approximation with a pairing residual interaction [13,14].

With the basis and the residual interaction thus chosen we proceed to evaluate the absolute decay width and the W -coefficients [14] as a function of the deformation parameters. It is known that, in even-even nuclei, deformations play an important role in alpha decay [13], although only the quadrupole and the hexadecapole deformations determine the absolute decay width. In the case of odd-mass nuclei that we study here a similar behavior is found for allowed transitions. For instance, one observes in Fig. 1 that the total width for the case of the odd-proton nucleus ^{207}At is strongly dependent upon the quadrupole deformation β_2 . The total width increases by about one order of magnitude by changing β_2 from 0 to +0.3 (i.e., for prolate deformations). A similar behavior is seen in this figure for negative quadrupole (oblate) deformations. However, as it was the case for even-even nuclei, the role of larger multiplicities on the total width is practically negligible. The influence of the deformation for the other At isotopes is very similar, as can be seen in Table I.

An even more pronounced effect of deformation on alpha decay can be seen for the nucleus ^{207}Rn , also presented in Fig. 1. The interesting feature of this case is that the mass number is the same as in the nucleus ^{207}At . It is only the odd neutron in Rn that produces the differences between the two cases. The calculated total decay widths as a function of β_2 for the other Rn isotopes are

reported in Table II.

The angular dependence of the emitted alpha particle is given by the corresponding emission probability. This is determined by the W -coefficients which, as seen in Ref. [14], are a superposition of all L -deformations through the coefficient A_L . In Fig. 2 we present the dependence of the coefficient A_L as a function of the quadrupole deformation for the odd-proton case of ^{207}At with $I_i = I_f = \frac{9}{2}$. The coefficient A_2 has positive values (in phase with $A_0=1$) for prolate deformations and negative values (opposite phase) for oblate ones. The other coefficients A_L with $L \neq 2$ are virtually negligible. For instance, the values of A_4 are one order of magnitude smaller than A_2 . In spite of this, it is interesting to note that A_4 is positive and symmetric with respect to the deformation parameter β_2 . A similar qualitative and even quantitative behavior is found for the other At isotopes, as can be seen in Table III. Actually even for the odd-neutron case of ^{207}Rn ($I_i = I_f = \frac{5}{2}$) and the other Rn isotopes all the features discussed above are essentially the same, as can be seen in Table IV.

The dependence of A_L versus deformation determines the corresponding behavior of the W -coefficients. Thus, one sees in Fig. 2 that the values of $W(\vartheta = 0^\circ)$ (solid line) and $W(\vartheta = 90^\circ)$ (dashed line) in the case of ^{207}At are strongly dependent upon quadrupole deformations, as was the case for the corresponding coefficient A_2 . The coefficient $W(\vartheta = 0^\circ)$ increases while $W(\vartheta = 90^\circ)$ decreases as a function of β_2 . Therefore our calculation predicts that the ratio $\mathcal{R} = W(0^\circ)/W(90^\circ)$ should be $\mathcal{R} < 1$ for oblate and $\mathcal{R} > 1$ for prolate deformations. It is worthwhile to point out that $\mathcal{R} \neq 1$ even for small deformations.

Practically identical results are found for other At isotopes, as can be seen in Table V, as well as for all Rn isotopes, as seen in Fig. 2 and Table VI.

We have so far analyzed the influence of quadrupole deformation on anisotropy. The corresponding deformation parameter β_2 is usually extracted from the elec-

TABLE II. Total widths (in MeV) in the case of Rn isotopes for different quadrupole deformations. Experimental widths (in MeV) from the compilation of Ref. [11].

$\beta_2 =$	-0.3	-0.2	-0.1	0.0	0.1	0.2	0.3	Γ_{exp}
$^{205}_{86}\text{Rn}$	1.8(-24)	1.1(-24)	7.8(-25)	6.7(-25)	8.0(-25)	1.4(-24)	3.3(-24)	6.2(-25)
$^{207}_{86}\text{Rn}$	2.3(-25)	1.4(-25)	9.8(-26)	8.5(-26)	1.0(-25)	1.8(-25)	4.2(-25)	1.9(-25)
$^{209}_{86}\text{Rn}$	1.2(-25)	7.4(-26)	5.1(-26)	4.4(-26)	5.3(-26)	9.2(-26)	2.2(-25)	4.6(-26)
$^{219}_{86}\text{Rn}$	4.7(-22)	3.0(-22)	2.1(-22)	1.8(-22)	2.2(-22)	3.6(-22)	8.1(-22)	8.6(-24)

TABLE III. The coefficient A_2 in the case of At isotopes for several values of the deformation.

$\beta_2 =$	-0.3	-0.2	-0.1	0.0	0.1	0.2	0.3
$^{201}_{85}\text{At}$	-1.048	-0.882	-0.566	0.000	0.776	1.479	1.912
$^{203}_{85}\text{At}$	-1.054	-0.889	-0.573	0.000	0.790	1.498	1.927
$^{205}_{85}\text{At}$	-1.057	-0.893	-0.578	0.000	0.799	1.510	1.937
$^{207}_{85}\text{At}$	-1.061	-0.897	-0.582	0.000	0.806	1.520	1.945
$^{209}_{85}\text{At}$	-1.063	-0.900	-0.585	0.000	0.812	1.528	1.951
$^{211}_{85}\text{At}$	-1.059	-0.895	-0.579	0.000	0.801	1.514	1.940

TABLE IV. The coefficient A_2 in the case of Rn isotopes for several values of the deformation.

$\beta_2 =$	-0.3	-0.2	-0.1	0.0	0.1	0.2	0.3
$^{205}_{86}\text{Rn}$	-0.750	-0.620	-0.388	0.000	0.512	0.978	1.279
$^{206}_{87}\text{Rn}$	-0.753	-0.630	-0.391	0.000	0.515	0.985	1.285
$^{209}_{86}\text{Rn}$	-0.754	-0.625	-0.392	0.000	0.518	0.989	1.290
$^{219}_{86}\text{Rn}$	-0.741	-0.609	-0.378	0.000	0.493	0.953	1.258

TABLE V. The coefficients $W(\vartheta)$ for $\vartheta = 0^\circ$ and $\vartheta = 90^\circ$ for At isotopes.

$\beta_2 =$	-0.3	-0.2	-0.1	0.0	0.1	0.2	0.3
	$W(0^\circ)$						
$^{201}_{85}\text{At}$	0.134	0.235	0.476	1.000	1.839	2.705	3.311
$^{203}_{85}\text{At}$	0.131	0.230	0.470	1.000	1.854	2.730	3.334
$^{205}_{85}\text{At}$	0.130	0.227	0.466	1.000	1.865	2.747	3.348
$^{207}_{85}\text{At}$	0.128	0.225	0.463	1.000	1.873	2.760	3.360
$^{209}_{85}\text{At}$	0.127	0.223	0.460	1.000	1.880	2.771	3.370
$^{211}_{85}\text{At}$	0.129	0.226	0.465	1.000	1.867	2.752	3.353
	$W(90^\circ)$						
$^{201}_{85}\text{At}$	1.593	1.485	1.299	1.000	0.635	0.346	0.194
$^{203}_{85}\text{At}$	1.596	1.489	1.303	1.000	0.629	0.339	0.189
$^{205}_{85}\text{At}$	1.599	1.492	1.305	1.000	0.625	0.334	0.186
$^{207}_{85}\text{At}$	1.601	1.494	1.308	1.000	0.622	0.330	0.183
$^{209}_{85}\text{At}$	1.603	1.496	1.309	1.000	0.620	0.327	0.181
$^{211}_{85}\text{At}$	1.600	1.493	1.306	1.000	0.624	0.333	0.185

TABLE VI. The coefficients $W(\vartheta)$ for $\vartheta = 0^\circ$ and $\vartheta = 90^\circ$ for Rn isotopes.

$\beta_2 =$	-0.3	-0.2	-0.1	0.0	0.1	0.2	0.3
	$W(0^\circ)$						
$^{205}_{86}\text{Rn}$	0.294	0.408	0.622	1.000	1.524	2.026	2.365
$^{207}_{86}\text{Rn}$	0.292	0.405	0.619	1.000	1.529	2.034	2.372
$^{209}_{86}\text{Rn}$	0.291	0.403	0.618	1.000	1.532	2.039	2.376
$^{219}_{86}\text{Rn}$	0.302	0.417	0.631	1.000	1.506	1.998	2.340
	$W(90^\circ)$						
$^{205}_{86}\text{Rn}$	1.392	1.320	1.197	1.000	0.750	0.529	0.393
$^{207}_{86}\text{Rn}$	1.393	1.322	1.199	1.000	0.748	0.526	0.390
$^{209}_{86}\text{Rn}$	1.394	1.323	1.200	1.000	0.746	0.524	0.388
$^{219}_{86}\text{Rn}$	1.387	1.314	1.193	1.000	0.758	0.541	0.402

TABLE VII. Deformations, experimental, and computed total widths, the coefficients $A_L, L=2,4$, the coefficients $W(\vartheta)$ for $\vartheta = 0^\circ$ and 90° and their ratios for realistic values of deformation within the chain of Rn isotopes.

	β_2	Γ_{exp}	Γ_{th}	A_2	A_4	$W(0^\circ)$	$W(90^\circ)$	$\frac{W(0^\circ)}{W(90^\circ)}$
$^{205}_{86}\text{Rn}$	0.005	6.16(-25)	6.76(-25)	0.022	0.000	1.022	0.989	1.034
$^{207}_{86}\text{Rn}$	0.016	1.90(-25)	8.50(-26)	0.076	0.000	1.076	0.962	1.118
$^{209}_{86}\text{Rn}$	0.023	4.56(-26)	4.27(-26)	0.111	0.001	1.112	0.944	1.177
$^{219}_{86}\text{Rn}$	0.081	8.61(-24)	2.05(-22)	0.398	0.008	1.406	0.804	1.749
$^{221}_{87}\text{Fr}$	0.069	2.40(-25)	1.08(-24)	-0.288	0.005	0.717	1.146	0.626

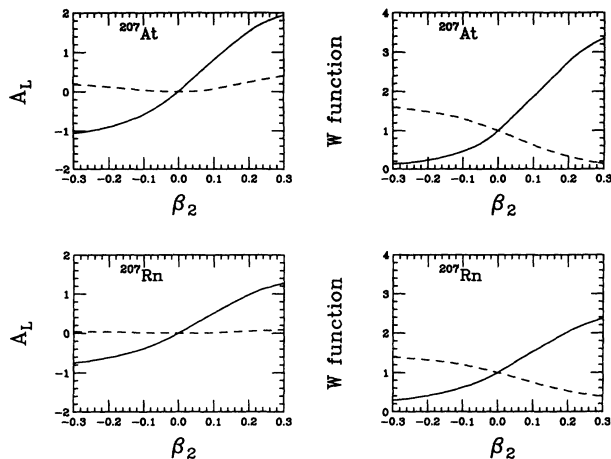


FIG. 2. The coefficients A_L for $L=2$ (solid line) and $L=4$ (dashed line) for the nuclei ^{207}At and ^{207}Rn as a function of the deformation. On the right side the coefficients $W(0^\circ)$ (solid line) and $W(90^\circ)$ (dashed line) versus deformation for ^{207}At and ^{207}Rn are also given.

tric quadrupole moment, which is a measurable quantity. This quantity has been measured for $^{205,207,209,219}\text{Rn}$ as well as for ^{221}Fr . In connecting quadrupole moments with β_2 we use the standard relation [17]

$$Q = Q_0 \frac{3K^2 - I(I+1)}{(2I+3)(I+1)}, \quad (1)$$

with Q_0 denotes the intrinsic quadrupole moment.

$$Q_0 = \frac{3}{\sqrt{5\pi}} R^2 \beta_2. \quad (2)$$

In our case we use for the parent nucleus $K = I = I_i$.

The computed deformations for $^{205,207,209,219}\text{Rn}$ and for ^{221}Fr are given in Table VII. In Fig. 3 we plotted the ratios \mathcal{R} for $^{205,207,209,219}\text{Rn}$ as a function of the deformation parameters extracted from experiment. One can see that even for small deformations there is an observable anisotropy. In the case of ^{219}Rn this effect is large, as expected. In this range of deformation the dependence of that ratio on the deformation is linear. In the same figure we plotted \mathcal{R} as a function of the same number. Corresponding numerical values are given in the Table VII.

Experimental values of the function $W(\vartheta)$ are affected by several experimental corrections [15]:

$$W(\vartheta) = 1 + \sum_{L=2,4} Q_L B_L U_L A_L P_L(\cos \vartheta). \quad (3)$$

Here A_L are the theoretical A -coefficients [14], Q_L are coefficients that take into account the dimensions of the source and detectors, B_L describe the orientations of the nuclei, and U_L correct B_L for unobserved intermediate transitions.

In the decay [14]

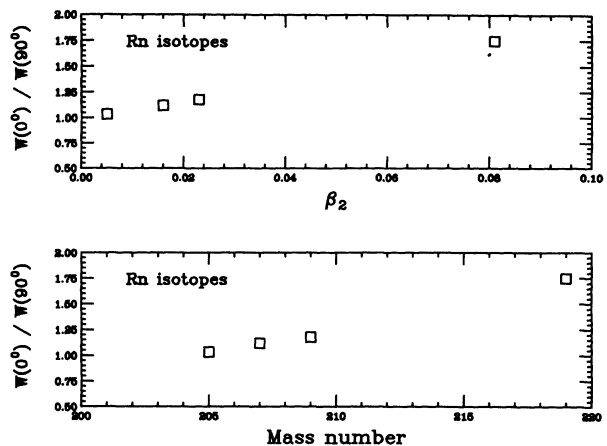
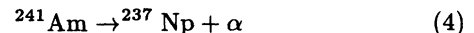


FIG. 3. The ratio $\mathcal{R} = W(0^\circ)/W(90^\circ)$ for Rn isotopes as a function of the deformation. In the lower part the same ratio for Rn isotopes as a function of the mass number is reported.



the overall correcting coefficient was found to be $Q_2 B_2 U_2 = 0.50$ for $\vartheta = 0^\circ$ and 0.52 for $\vartheta = 90^\circ$ for quadrupole deformations while the contribution of hexadecapole and higher deformations is negligible. One can expect the same experimental corrections in the cases analyzed in this paper.

In conclusion, we have presented, in the present paper, a systematic microscopic calculation of quantities related to alpha particle emission from oriented odd-mass At and Rn isotopes at low temperature. We emphasized in this study the importance of anisotropies in alpha decay processes as a tool to extract intrinsic deformation parameters in nuclei. In order to describe correctly the asymptotic behavior of the formation amplitude we used a large single-particle basis. We found that the probability of emitting an alpha particle in the polar direction with respect to the corresponding probability in the equatorial direction is strongly dependent on the emission angle. For prolate deformations that ratio is greater than one, while for oblate deformations it is less than one. We also found that deformations higher than quadrupole do not play any significant role in the emission probability. Even for near spherical nuclei the anisotropy was found to be measurable. The importance of this result is that it can shed some light on the problem of determining deformation parameters from experimentally extracted quantities. We did this by using measured quadrupole moments, as usual. We adopted for the corresponding calculation the Bohr-Mottelson liquid drop model. But the value of the deformation parameter β_2 may be different if one uses other models. For instance, within the alpha-core coupling used in Ref. [10] the relation between quadrupole moment and β_2 is different from the relation given in Eq. (1). Therefore, the experimental determination of anisotropies in alpha particle emission is important to clarify this old but still timely problem.

- [1] S. H. Hanauer, J. W. T. Dabbs, L. D. Roberts, and G. W. Parker, *Phys. Rev.* **124**, 1512 (1961); Q. O. Navarro, J. O. Rasmussen, and D. A. Shirley, *Phys. Lett.* **2**, 353 (1962).
- [2] A. J. Soinski, R. B. Frankel, Q. O. Navarro, and D. A. Shirley, *Phys. Rev. C* **2**, 2379 (1970).
- [3] A. J. Soinski and D. A. Shirley, *Phys. Rev. C* **10**, 1488 (1974).
- [4] D. Vandenplassche, E. van Walle, C. Nuytten, and L. Vanneste, *Phys. Rev. Lett.* **49**, 1390 (1982).
- [5] F. A. Dilmanian *et al.*, *Phys. Rev. Lett.* **49**, 1909 (1982).
- [6] J. Wouters, D. Vandenplassche, E. van Walle, N. Severijns, and L. Vanneste, *Phys. Rev. Lett.* **56**, 1901 (1986); *Nucl. Instrum. Methods B* **26**, 463 (1987); N. G. Nicolis *et al.*, *Phys. Rev. C* **41**, 2118 (1990).
- [7] D. L. Hill and J. D. Wheeler, *Phys. Rev.* **89**, 1102 (1953).
- [8] P. O. Fröman, *K. Dan. Vidensk. Selsk. Mat.-Fys. Skr.* **1**, No. 3 (1957); A. Bohr, P. O. Fröman, and B. Mottelson, *K. Dan. Vidensk. Selsk., Mat.-Fys. Medd.* **29**, No. 10 (1955).
- [9] T. Berggren, *Phys. Lett. B* **197**, 1 (1987); *Hyperfine Interact.* **43**, 407 (1988).
- [10] T. Berggren, Report No. Lund-MPh-93/14; private communication.
- [11] B. Buck, A. C. Merchant, and S. M. Perez, *J. Phys. G* **18**, 143 (1992). *At. Data Nucl. Data Tables* **54**, 53 (1993).
- [12] N. Rowley, G. D. Jones, and M. W. Kermode, *J. Phys. G* **18**, 165 (1992).
- [13] A. Insolia, P. Curutchet, R. J. Liotta, and D. S. Delion, *Phys. Rev. C* **44**, 545 (1991); D. S. Delion, A. Insolia, and R. J. Liotta, *ibid.* **46**, 1346 (1992).
- [14] D. S. Delion, A. Insolia, and R. J. Liotta, *Phys. Rev. C* **46**, 884 (1992).
- [15] P. Schuurmans *et al.*, Report No. CERN/ISC 93-3, 1993.
- [16] R. Bengtsson, J. Dudek, W. Nazarewicz, and P. Olanders, *Phys. Scr.* **39**, 196 (1989); S. Cwiok, J. Dudek, W. Nazarewicz, J. Skalski, and T. Werner, *Comput. Phys. Commun.* **46**, 379 (1987).
- [17] A. Bohr and Mottelson, *Nuclear Structure* (Benjamin, New York, 1975), Vol. 2.